



HAL
open science

Wettability and surface forces measured by atomic force microscopy: the role of roughness

J. Gavaille, J. Takadoum, N. Martin, D. Dominique Durand

► To cite this version:

J. Gavaille, J. Takadoum, N. Martin, D. Dominique Durand. Wettability and surface forces measured by atomic force microscopy: the role of roughness. *European Physical Journal: Applied Physics*, 2009, 48 (1), pp.1-5. 10.1051/epjap/2009120 . hal-00497323

HAL Id: hal-00497323

<https://hal.science/hal-00497323>

Submitted on 4 Jul 2010

HAL is a multi-disciplinary open access archive for the deposit and dissemination of scientific research documents, whether they are published or not. The documents may come from teaching and research institutions in France or abroad, or from public or private research centers.

L'archive ouverte pluridisciplinaire **HAL**, est destinée au dépôt et à la diffusion de documents scientifiques de niveau recherche, publiés ou non, émanant des établissements d'enseignement et de recherche français ou étrangers, des laboratoires publics ou privés.

Wettability and surface forces measured by atomic force microscopy:

The role of roughness

J. Gavaille, J. Takadoum, N. Martin, D. Durand*

FEMTO-ST. CNRS, Université de Franche-Comté, ENSMM, UTBM

26, chemin de l'épitaphe, 25030 Besançon, France

Abstract

Thin films of titanium, copper and silver with various roughnesses were prepared by physical vapour deposition technique: dc magnetron sputtering. By varying the deposition time from few minutes to one hour it was possible to obtain metallic films with surface roughness average ranging from 1 to 20 nm. The wettability of these films was studied by measuring the contact angle using the sessile drop method and surface forces were investigated using the atomic force microscopy (AFM) by measuring the pull-off force between the AFM tip and the surfaces. Experimental results have been mainly discussed in terms of metal surface reactivity, Young modulus of the materials and real surface of contact between the AFM tip and the film surfaces.

Keywords: surface forces, adhesion, wettability, thin films, sputtering, AFM

** Corresponding author ; tel : +33 (0)3 81 40 28 69 ; fax : +33 (0)3 81 40 28 52 ;*

e-mail : joseph.gavoille@ens2m.fr

1. Introduction

The versatility of the films prepared by physical vapour deposition (PVD) allows them to be used in various domains such as optics, microelectronics, decorative industry or mechanics. The comprehension of the physico-chemical properties of such coatings is of great importance to enlarge their domains of application and improve their knowledge and use. In particular, the use of such materials in micromechanical devices [1-2] are especially attractive because, at this scale, the material behaviour is much more influenced by the surface characteristics than by the bulk material properties. Thus, the preparation of surfaces with particular properties (wear, friction, chemistry) becomes important. Moreover, in such devices, physico-chemical properties of surfaces influence their mechanical performance since a growing part of contact forces is due to adhesion while the scale is reduced. Theories describing the surface forces occurring when two surfaces are in contact imply that the surfaces are perfectly smooth [3-4]. Nevertheless materials surfaces are rough, which leads to a real contact area composed from contact microspheres grouped into contact spots.

In the particular case of surfaces prepared by PVD techniques, it is possible to obtain surfaces with controlled roughness by depositing films of different thicknesses [5]. One can achieve surface roughness average (R_a) values ranging from 1 nm to 20 nm when deposition time varies from few minutes to one hour.

In order to show the influence of surface roughness on surface force measured by atomic force microscopy (AFM), thin metallic films (Ti, Ag, Cu) with various microgeometric profiles were prepared. The influence of the topography (roughness, nodules area) and Young modulus of the materials on wettability and adhesion was analysed.

2. Materials and methods

The deposition of metallic thin films was performed in a home-made high vacuum reactor, whose volume was approximately 60 L. Titanium, copper and silver coatings were sputter deposited on glass substrates at room temperature (293 K) from metallic targets of 5 cm diameter with an argon pressure kept constant at 0.5 Pa during the deposition process. Depending on the nature of the deposited metal (and consequently its sputtering yield), the deposition time was adjusted in order to obtain films with various thicknesses (from 100 to 1500 nm) and surface roughness values (Ra ranging from 1 to 20 nm).

Surface morphology of the films was studied using a Nanoscope III (Digital Instruments) atomic force microscope (AFM). The surface roughness average (Ra) of the films was determined on three different regions of $1 \mu\text{m}^2$ area and the results were averaged to obtain the values reported in Table 1. The atomic force microscope was also used to study surface forces. Adhesion between the tip of the AFM and a sample surface was monitored as a function of the displacement of the sample relative to the tip. Figure 1 shows a schematic force curve during an extension-retraction cycle of the AFM piezoelectric motor. Force versus distance curves were acquired in order to reveal the interaction between the surface of the sample and the tip of the AFM. These curves permit the determination of the adhesion force between the tip and the sample surface. It is equal to the necessary force to elastically deform the cantilever during the jump off contact. During the retraction of the piezoelectric motor, the contact breaks when the elastic force due to the deflexion of the cantilever, overpasses the adhesion force between the tip and the surface. The tip used was a silicon nitride (Si_3N_4) standard V-shaped cantilever tip provided by Digital Instruments, with a 200 nm tip radius and a $0.3 \text{ N}\cdot\text{m}^{-1}$ spring constant. In order to avoid the influence of the adsorbed water layer on the surfaces and thus the meniscus force between the tip and the sample surface, the

experiments were carried out in ethanol using a cell fluid apparatus. Ethanol is commonly used because of its lack of ionic strength.

The crystallographic structure and the average grain size of the films were investigated by X-rays diffraction (XRD). A Siemens FF CU 4KE diffractometer equipped with a monochromatised Cu K_{α} radiation source in the $\theta/2\theta$ configuration was used. The adhesion force between the tip and the sample surface was calculated taking into account the elastic constant of the cantilever (k) and the total deflexion (δ) of the cantilever to necessary break the contact force between the tip and the surface of the sample. Such a force depends on the nature of the surfaces and on the geometry of the contact.

Surface energy γ_s of the coatings was determined by measuring contact angle θ using the sessile drop method. The Chaudhury Good van Oss [6] decomposition of the surface energy γ_s was used:

$$\gamma_s = \gamma_s^{LW} + 2\sqrt{\gamma_s^+ \gamma_s^-} \quad (1)$$

where γ_s^{LW} is the apolar (Lifshitz van der Waals) surface tension component (mJ), γ_s^+ and γ_s^- the electron-acceptor and donor surface tension parameters (mJ) according to the Lewis acid-base theory.

3. Results and discussion

With a room substrate temperature (293K) and at low argon pressure (few tenths of Pa), metallic thin films sputter deposited are usually composed of thin columns separated by voids, which corresponds to the zone 1 of the Thornton's structural model [7]. The typical island growth (Volmer-Weber-like mode [5]) implies that the roughness and nodules area of the surface increase with the thickness of the films and deposition time. Actually, small islands are formed at the beginning of the deposition process (first growing stages [8]), and with

increasing deposition time, coalescence of these islands occurs to form much bigger islands on the surface. AFM micrographs of the films surface show that coatings present a typical nodular surface morphology (Fig. 2). It is in agreement with the columnar growth expected by the Thornton's model. These figures clearly illustrate that nodules area increases with the thickness of the film (the nodules area of the surfaces was calculated by image analysis of the AFM micrographs). The range of average surface roughnesses achieved varied from 1 nm up to 20 nm depending on the deposition time and the nature of the material. Table 1 summarizes the values of surface roughness average (R_a), thickness (e) and nodules area (A), respectively, to the experimental deposition time (t) for the three tested materials. Because of the high sputtering yield (Y) of copper and silver ($Y_{Cu} = 1.65$, $Y_{Ag} = 2.55$ and $Y_{Ti} = 0.35$ for Xe^+ ions energy of 400 eV ([9]) these metals need lower deposition time than titanium to achieve comparable thickness (two times lower for copper and nearly six times lower for silver compared to titanium) (Table 1). X-rays diffraction patterns of the films deposited at room temperature on glass substrates show that the films are well-crystallised. Copper and silver are strongly (111) textured whereas titanium is (002) textured (Fig. 3). The crystallite size was estimated by the Scherrer's method and the results are reported in Fig. 4. As expected, crystallite size increases with the film thickness [10]. It is worth to note that calculations were only performed for thicknesses above 200 nm for which Scherrer's method becomes significant.

The influence of the topography of the films on the contact angle was previously studied [11-14]. It was shown that, increasing roughness may favour or reduce wettability depending on the nature of the surface. Uelzen and Müller [15] claim that wettability of smooth hydrophilic surfaces is improved by roughening them whereas a reverse effect is observed with smooth hydrophobic surfaces. In the present study, the cosine of the contact angle θ exhibits a linear dependency with the roughness (R_a) of the surface (Fig. 5). By increasing the roughness of the

surfaces, wettability is increased as well. Thus, contact angle θ decreases when the roughness increases. This result is in agreement with those reported for gold coatings by Uelzen and Müller [15].

Observations on the evolution of the cosine of the wet angle for a fixed value of R_a show that the cosine of the contact angle rises in the same order as the surface energy of metal ($\gamma_s(\text{Ag}) < \gamma_s(\text{Cu}) < \gamma_s(\text{Ti})$) (see inset in Fig. 5). This is in complete agreement with the correlation between the surface energy of materials and their wettability. Actually a very reactive metallic surface corresponds to a high wettability and thus a low contact angle.

It is well known that the real contact between two surfaces is the sum of microspheres, generally grouped into contact spots due to roughness. Since adhesion between surfaces is directly linked to the real area of contact (the higher the real area of contact, the better the adhesion) [3, 16], a reduction of the adhesion force measured by AFM is expected while the surface roughness increases. In our case, the opposite behaviour occurs. In fact, the rise of the surface roughness average of the surface is a consequence of a larger size of the nodules on the surface. While the top of the nodules are considered as spheres, the increasing size corresponds to an increasing radius of the counter surface relatively to the tip. The Rumpf's model [17] used for the calculation of the adhesion force F_{ad} (N) between two spheres is given by:

$$F_{\text{ad}} = \frac{A}{6H_0^2} \left[\frac{rR}{r+R} + \frac{R}{\left(1 + \frac{r}{H_0}\right)^2} \right] \quad (2)$$

where R is the radius of the tip (200 nm), A the Hamaker constant (J), H_0 the distance of closest approach (m) between surfaces and r the radius (m) of the asperity (considered as hemispherical). The first term represents the “contact” force between the two particles while

the second one represents the “non contact” force. A first approximation of this model shows that adhesion force between the two spheres increases with the radius of the asperity r .

Actually the geometry of the contact between the tip and the surface greatly depends on the surface topography. Regarding to the tip geometry and dimension (sphere with a radius of 200 nm), the nodules on the surface of the films change from sphere-like shape to plan since their size increases with deposition time. Thus, the deflexion of the cantilever vs. the surface of the nodules (Fig. 6) reveals two types of interaction. In zone 1 (surface of nodules lower than 10^4 nm^2), the adhesion increases because of the increasing area of contact (sphere / sphere contact). In zone 2 (surface of nodules higher than $2 \times 10^4 \text{ nm}^2$), the nodules are barely plan comparing to the AFM tip (sphere / plan contact) and one can see an asymptotic behaviour of the deflexion (adhesion) value. It tends to 4, 6 and 12 nm for titanium, copper and silver, respectively. This is in agreement with the relation (2). While the radius of the asperities on the surface becomes much greater than the radius of the tip ($r \gg R$) the “non contact” term tends to zero and the “contact” term tends to a finite value. Actually, adhesion force may be expressed by:

$$F_{\text{ad}} = \frac{AR}{6H_0^2} \quad (3)$$

Relation (3) shows that adhesion does not still depend on the surface roughness since the term (r) disappears. Consequently, for high r/R ratio values, F_{ad} remains constant as can be seen in figure 6. In this figure, it clearly appears that adhesion increases quite sharply for surface of nodules lower than 10^4 nm^2 whereas it tends asymptotically to a constant value for nodules surface higher than $2 \times 10^4 \text{ nm}^2$.

Since the contact between the tip of the AFM and the film surface is mainly elastic due to the low contact force involved, the elastic modulus of the material can be an important factor. Contact surface (and consequently F_{ad}) may be greatly affected by elastic modulus of the films. For silver (Young modulus $E = 80 \text{ GPa}$) elastic deformation (and consequently the size

of contact surface) during loading (extension of the AFM piezoelectric motor) is higher than for copper and titanium whose Young modulus is about 120 GPa. This tends to increase deflexion (the contact force) measured by AFM.

4. Conclusion

Wettability and surface forces (adhesion) investigated by atomic force microscopy were measured on the surface of three metallic thin films: Ti, Cu, Ag. Films were sputter deposited during times ranging from few minutes to one hour in order to obtain different surface roughnesses.

One can conclude from the above results that mechanical characteristics of the films as well as their roughness and their physico-chemical properties may act simultaneously and affect adhesion force measured by AFM. Nevertheless, the effect of roughness may be neglected when asperities on the surface become much greater than the radius of the tip ($r \gg R$).

The main results obtained may be summarized as follows:

- The adhesion force increases with surface roughness,
- The cosine of the contact angle rises in the same order as the surface energy of metal ($\gamma_s(\text{Ag}) < \gamma_s(\text{Cu}) < \gamma_s(\text{Ti})$) and is highly affected by the surface roughness. The contact angle relates to the surface roughness such as the rougher surface is, the less important contact angle is,
- Young modulus of the films may affect greatly adhesion measurements.

References

1. X. Li, B. Bhushan, K. Takashima, C.-W. Baek, Y.K. Kim, *Ultramicroscopy* **97**, 481 (2003)
2. S. Sundararajan, B. Bhushan, *Wear* **217**, 251 (1998)
3. K.L. Johnson, K. Kendall, A.D. Roberts, *Proc. R. Soc. London, A: Math. Phys. Sci.* **324**, 301 (1971)
4. B.V. Derjaguin, V.M. Muller, Y.P. Toporov, *J. Colloid Interface Sci.* **53** 314 (1975)
5. K. Reichelt, *Vacuum* **38(12)**, 1083 (1988)
6. C. J. van Oss, R. J. Good, M. K. Chaudhury, *Langmuir* **4**, 884 (1988)
7. J.A. Thornton, *J. Vac. Sci. Technol.* **11(4)**, 666 (1974)
8. V.I. Trofimov, *Thin Solid Films* **428**, 56 (2003)
9. P. Sigmund, *Phys. Rev.* **184**, 383 (1969)
10. B. Chapman , *Glow Discharge Processes* (John Wiley & Sons, New York, 1980)
11. H. Nakae, R. Inui, Y. Hirata, H. Saito, *Acta Mater.* **46(7)**, 2313 (1998)
12. E.R. Beach, G.W. Tormoen, J. Drelich, R. Han, *J. Colloid Interface Sci.* **247**, 84 (2002)
13. R.N. Wenzel, *Ind. Eng. Chem. Soc.* **74**, 988 (1936)
14. A. Feng, B.J. McCoy, Z.A. Munir, D. Cagliostro, *Mater. Sci. Eng.* **A252**, 50 (1998)
15. T. Uelzen, J. Müller, *Thin Solid Films* **434**, 311 (2003)
16. D. Tabor, *J. Colloid Interface Sci.* **58**, 2 (1977)
17. Y.I. Rabinovich, J.J. Adler, A. Ata, R.K. Singh, B.M. Moudgil, *J. Colloid Interface Sci.* **232**, 10 (2000)

Figure captions

Figure 1: schematic deflection versus position curves, which corresponds to an extension-retraction cycle of the AFM piezoelectric motor. AB is the total deflexion corresponding to the adhesion between the tip and the surface.

Figure 2: Surface topography by AFM of copper coatings for various thicknesses: a) 150nm; b) 450 nm; c) 900 nm.

Figure 3: X-rays diffraction patterns of copper, silver and titanium (thickness of the films is 900 nm).

Figure 4: grain size (by the Scherrer's method) as a function of the thickness of the films. Dotted line is a guide for the eyes.

Figure 5: cosine of the contact angle θ vs. roughness average R_a of the films. Surface energy γ_s is given for comparison. Dotted line is a guide for the eyes.

Figure 6: Deflexion of the AFM cantilever vs. nodules area at the surface of the films. Dotted line is a guide for the eyes.

Table 1: thickness (e), deposition time (t), roughness (R_a) and nodules area (A) of the prepared films.

	e (± 20 nm)	t (min)	R_a (± 0.1 nm)	A (± 100 nm²)
Titanium	180	15	3.2	6×10^2
	250	30	6.7	5×10^3
	460	60	7.0	9.5×10^3
	690	90	5.5	1.51×10^4
	1500	180	11.8	2.9×10^4
Copper	150	8	1.5	4×10^3
	220	13	4.5	6.1×10^3
	440	24	6.0	1.19×10^4
	700	36	13.1	1.39×10^4
	860	45	19.7	2.34×10^4
Silver	100	2.5	2.3	2.4×10^3
	450	10	2.3	5.5×10^3
	680	15	5.0	1.29×10^4
	1470	32.5	5.6	2.84×10^4

Figure 1

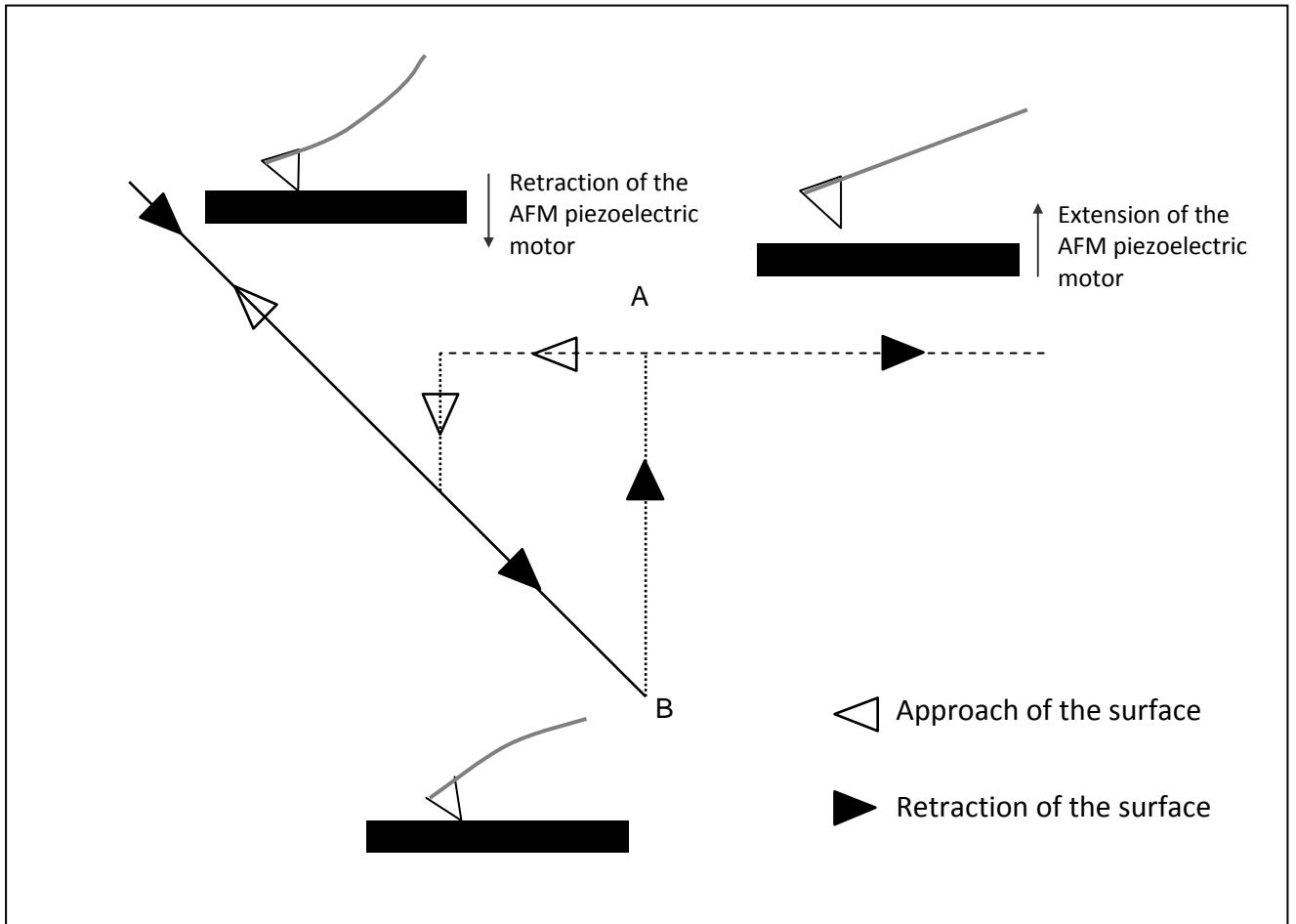


Figure 2 (1/2)

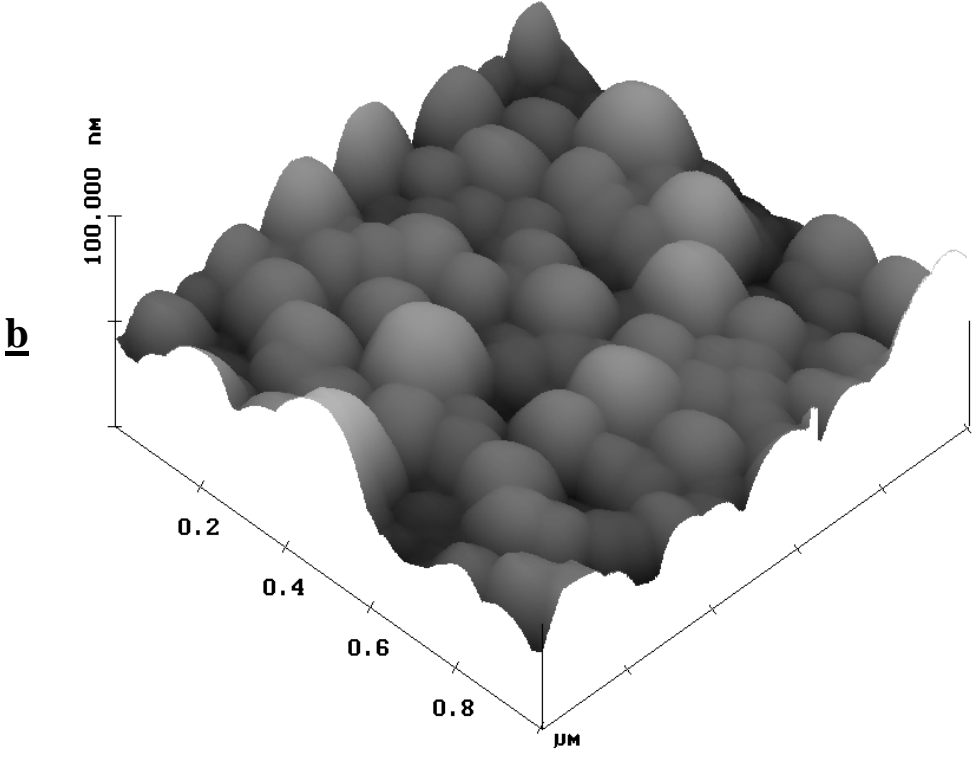
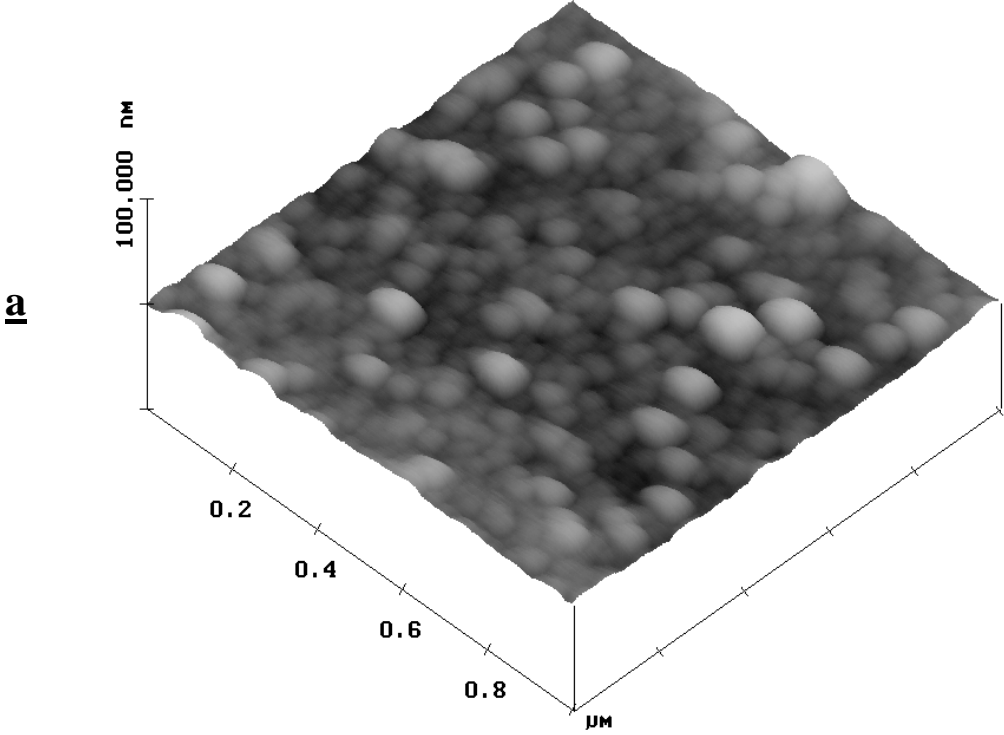


Figure 2 (2/2)

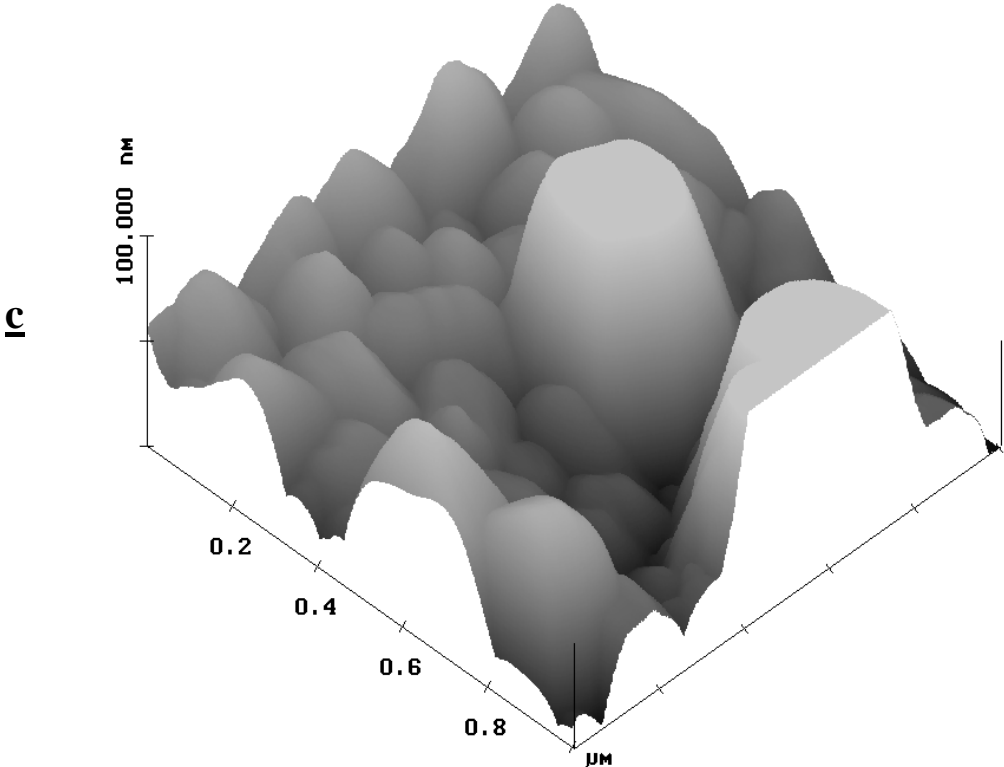


Figure 3

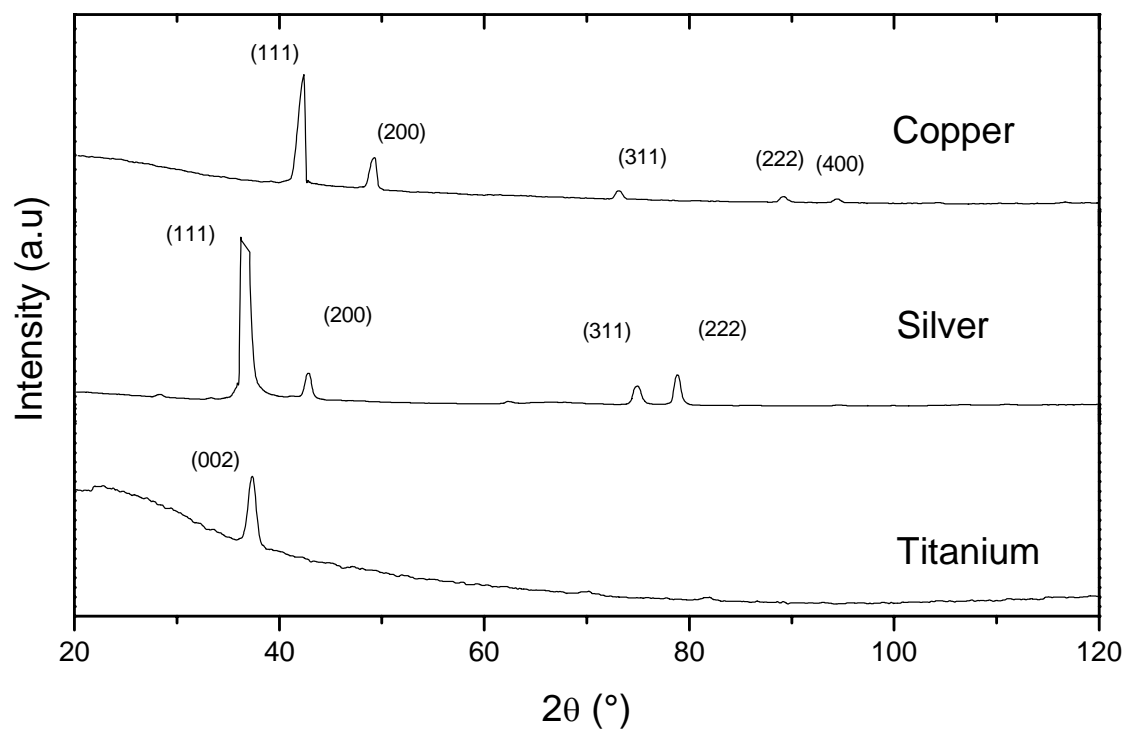


Figure 4

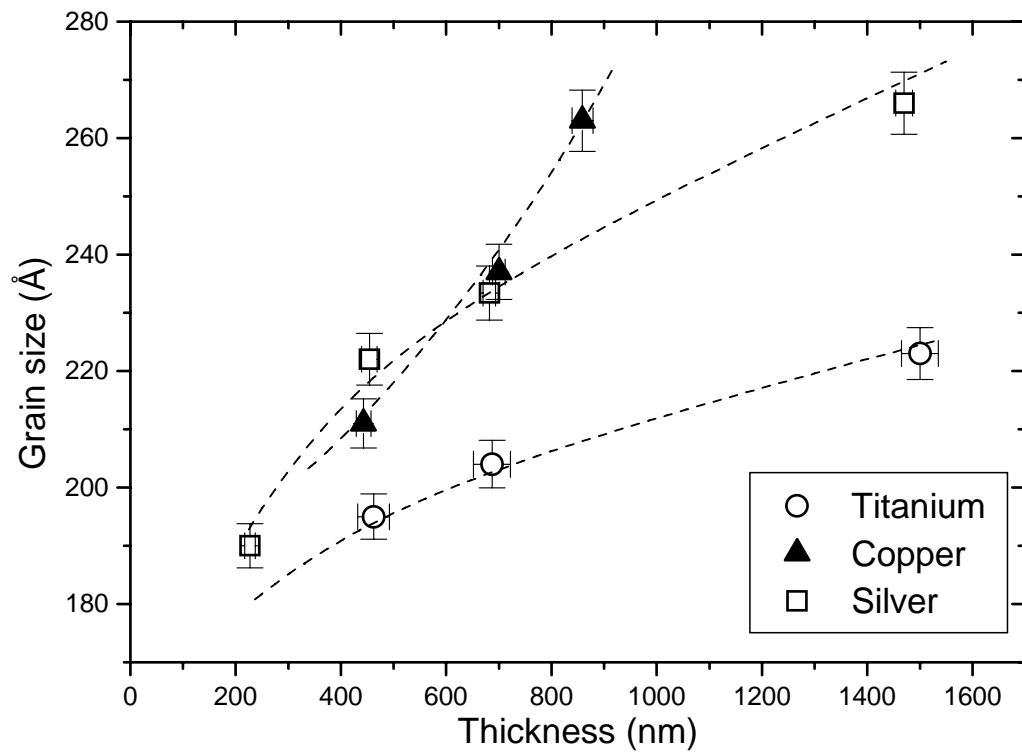


Figure 5

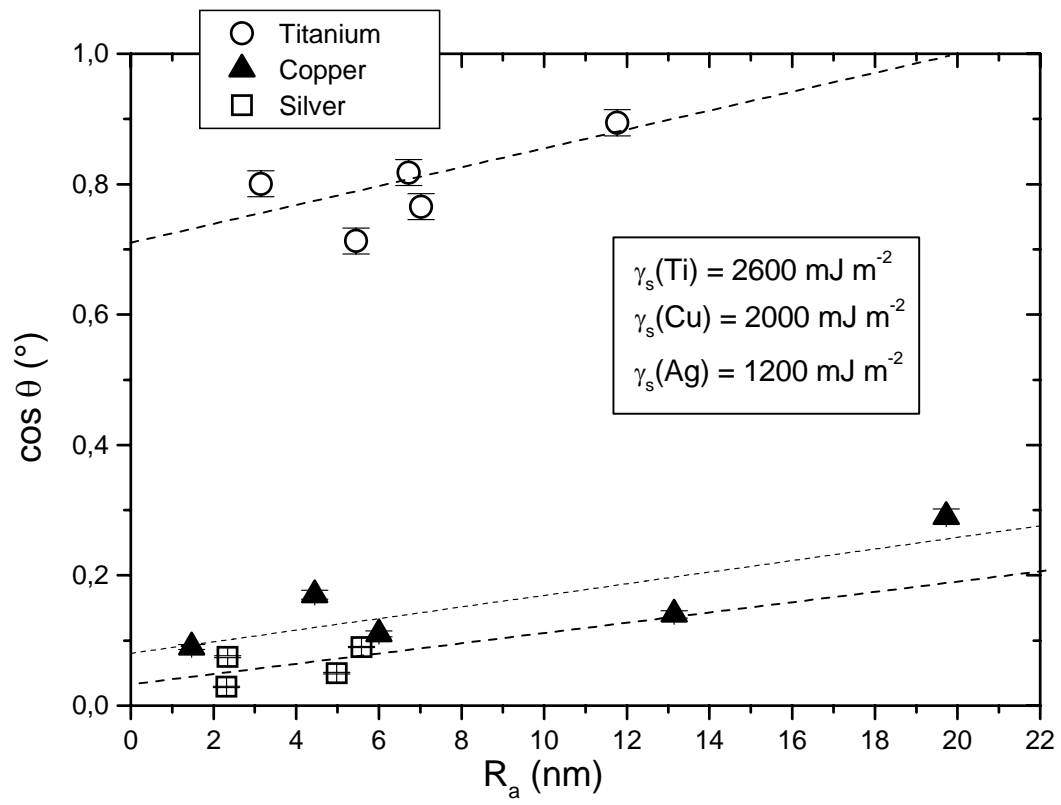


Figure 6

